Available online at www.sciencedirect.com

ScienceDirect

Procedia Structural Integrity 42 (2022) 623–630

Structural Integrity Procedia

www.elsevier.com/locate/procedia

23 European Conference on Fracture - ECF23

Frequency Effects in Ultrasonic Fatigue Testing (UFT) of Q355B Structural Steel

Lewis Milne[a,]*, Yevgen Gorash[a], Tugrul Comlekci[a], Donald MacKenzie[a]

[a]*Dept. of Mechanical and Aerospace Engineering, University of Strathclyde, 75 Montrose Street, Glasgow, G1 1XJ, UK*

Abstract

Ultrasonic Fatigue Testing (UFT) is an accelerated fatigue testing method, capable of running at 20 kHz. This increased test frequency can have significant influence on the results produced for ferritic steels due to the strain rate sensitivity of the deformation mechanisms and internal heat dissipation. The aim of this investigation was to evaluate the frequency effect for the structural steel Q355B. To achieve this, the fatigue performance of the material was evaluated at 20 Hz and at 20 kHz using a test method designed to reduce the variables between the tests to just the load frequency. The discrepancy between the SN curves produced at the two frequencies was evaluated and found to match well with similar steels in literature. The effect of the ferrite content on the frequency sensitivity was evaluated, and the heat generation and fracture origin within the samples was discussed. The observations for each of these matched similar observations in literature.

Keywords: ultrasonic fatigue testing; very high cycle fatigue; structural steels; frequency effect; strain rate effects

1. Background

Ultrasonic Fatigue Testing (UFT) is an accelerated method of fatigue testing in which piezoelectric actuators are used to vibrate a test specimen at its resonant frequency, thereby inducing a cyclic load at a frequency of 20 kHz (Bathias 2006). This high test frequency enables the fatigue testing of materials well beyond the traditional fatigue

* Corresponding author. Tel.: +44 07578 951 319.
E-mail address: lewis.milne.2015@uni.strath.ac.uk

10.1016/j.prostr.2022.12.079

limit of 10^7 cycles, into what is known as the Very-High Cycle Fatigue (VHCF) regime. Depending on the material being tested, however, the increased test frequency inherent in UFT can have a significant influence on the produced fatigue results. In particular, for Body-Centred Cubic (BCC) based materials, such as ferritic steels, the increased test frequency will induce two significant challenges which must be considered:

Firstly, the deformation mechanisms in BCC structures are sensitive to strain rate. At higher strain rates, the lattice friction stresses within the material will increase, leading to higher flow stresses being necessary to achieve dislocation glide (Mughrabi et al. 1981). As a result, ferritic materials will appear to be much stronger at higher test frequencies (Guennec et al. 2014; Klusák et al. 2021; Liu et al. 2016; Nonaka et al. 2014; Tsutsumi et al. 2009).

Secondly, the mechanical energy input to the material during cycling will be dissipated as heat. As UFT is carried out at a high frequency, this rate of energy dissipation will also be high, leading to rapid internal heat generation (Torabian et al. 2017). For ferritic steels, this can generate hundreds of degrees, even when intermittent loading and air cooling are applied (Gorash et al. 2022). As of yet, there is no reliable method to relate the fatigue data for ferritic steels produced through UFT to the data produced at traditional frequencies, and until this is achieved, the usability of UFT for these materials is limited.

Some attempts to quantify this frequency effect in literature are described below.

Gorash et al. (2022) evaluated the average discrepancy between the SN curves produced at 20 kHz and 20 Hz for the structural steel S275JR. This provided a simple method of evaluating the strain rate sensitivity for a given material.

Bach et al. (2018) investigated the effect of ferrite content on the frequency effect across a range of carbon steels using an adaptation of the Hart equation. It was observed that the discrepancy between the SN curves at 20 kHz and at 110 Hz appeared to strongly correlate with the ferrite volume %. The ferrite content was therefore identified as an important factor which must be considered when evaluating the frequency effects in steels.

Hu et al. (2018) proposed the use of the Johnson-Cook equation to evaluate the frequency effect of a high-strength steel, by quantifying the effect of strain rate on the material's yield strength. Although this relation worked well for the investigated high-strength steel, it has yet to be applied to ferritic steels.

Guennec et al. (2015) attempted to compare the SN curves at ultrasonic and standard frequencies for S15C steel by creating a frequency-insensitive master curve. This was achieved by normalizing the SN curves produced at a range of different test frequencies using the yield strength at the corresponding strain rate for each frequency. It was found that this approach worked well for the lower frequencies tested (from 0.2 Hz to 140 Hz), however, there was still a significant discrepancy between the UFT curve and the other SN curves. The reason proposed for this was the transition from athermal dislocation glide at low frequencies to thermally activated glide at the ultrasonic frequencies within the ferrite regions.

2. Aims

The aim of this investigation was to evaluate the frequency effect for the structural steel Q355B. To achieve this, the fatigue performance of the material was evaluated at 20 Hz and at 20 kHz using a test method designed to reduce the variables between the tests to just the load frequency. The same gauge section geometry was used for both frequencies and both materials were tested at room temperature. The effect of the frequency on the fatigue behaviour was then evaluated by quantifying the discrepancy between the two SN curves.

3. Methodology

3.1. Material Properties

The material tested was a Q355B steel plate of 12 mm thickness. Q355B is a mild ferritic-pearlitic steel with a nominal yield strength of 355 MPa. The chemical composition according to the quality certificate is given in Table 1.

Table 1: Chemical Composition Q355B according to the quality certificate (wt.%)

Material	C	Si	Mn	S	P	Fe
Q355B	0.17	0.34	1.40	0.012	0.016	Bal.

3.2. Test Specimen Design

As discussed by Fitzka et al. (2021), it is important to ensure that the risk volume of the specimen which is subjected to the peak stress amplitude is equivalent between all tested frequencies to avoid the influence of size effects. In order to achieve this, specimens with the exact same gauge geometry were produced for both 20 kHz and 20 Hz frequency testing, thereby eliminating any variation in geometrical effects between the experiments. As the ultrasonic specimen has tighter geometrical requirements to achieve resonance at 20 kHz, it was designed first, followed by the low-frequency specimen to match it.

The UFT specimens were designed according to the standard hourglass geometry described by the UFT standard WES 1112 (2017). To tune the specimen's resonant frequency to exactly 20 kHz, the shoulder length was adjusted following a harmonic analysis in ANSYS Workbench. The final specimen geometry is given in Figure 1 (a). After manufacturing, the resonant frequency of the physical samples was tested using the Shimadzu USF-2000A machine and found to be 20.05 kHz, which lies well within the machine's working range of 19.5-20.5 kHz.

The 20 Hz specimen was designed to have the same hourglass gauge geometry, but with longer shoulders to allow gripping with a servohydraulic test machine. The specimen geometry is shown in Figure 1 (b).

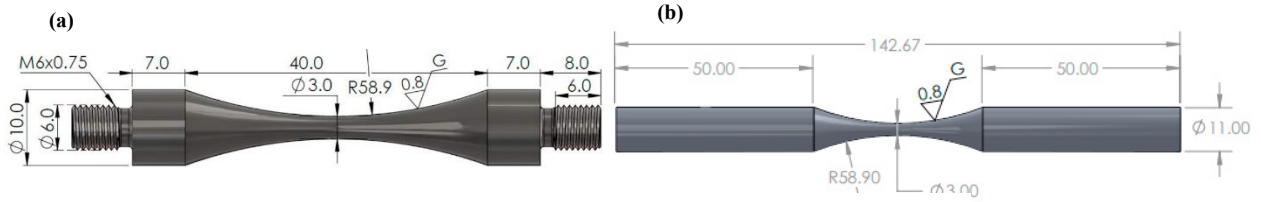

Figure 1: Specimen Dimensions of (a) the 20 kHz test and (b) the 20 Hz test

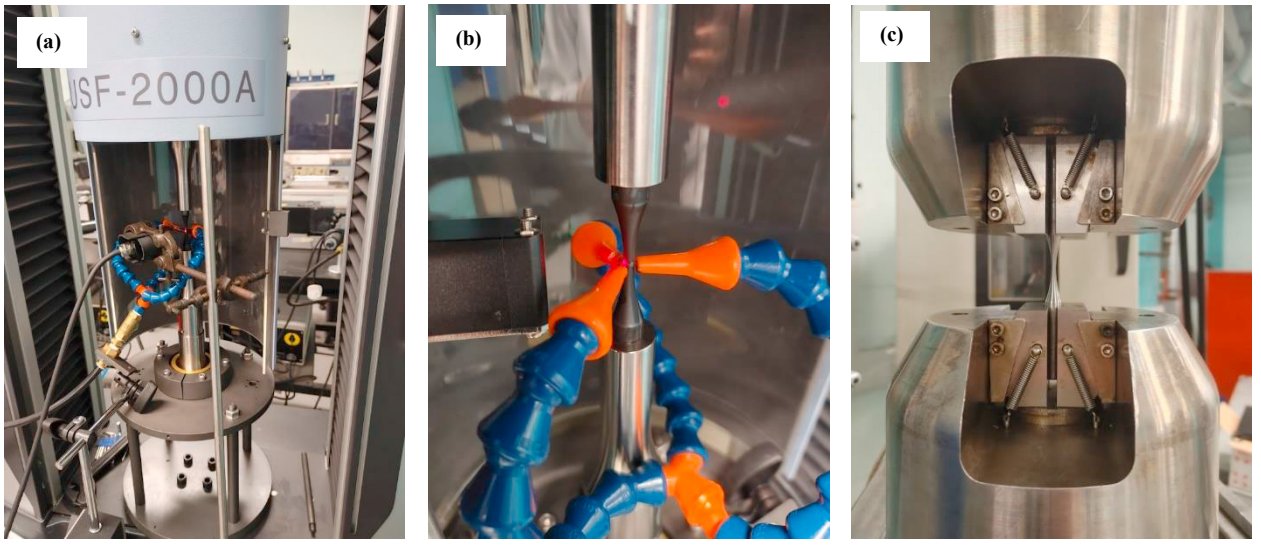

Figure 2: Test specimens in the Shimadzu USF-2000A Testing machine (a,b), and Instron 8801 Servohydraulic test machine (c)

3.3. Test Procedure

The high-frequency testing was carried out at 20 kHz using a Shimadzu USF-2000A ultrasonic testing machine. Threads were used to attach the specimen to acoustic horns on both sides and the height of the top horn was adjusted to achieve zero mean stress. The automatic fracture detection feature was enabled, which stops the test when a crack is formed by monitoring the change in the resonance frequency.

To cool the specimen, forced air convection was applied using cooling nozzles blowing compressed dried air over the sample, and intermittent load pulses were used. The loading pulse was kept at 110 ms, and the cooling pause was adjusted between 0.5-5 s depending on the rate of heat generation. This allowed the test duration to be minimised by using shorter cooling pauses near the beginning of the test when there was little heat generation, while utilising longer cooling pauses towards the end when the heat generation was greater. Specimens were painted with a high emissivity black paint, and an infrared (IR) spot sensor with a sampling interval of 20 ms was used to monitor the specimen temperature. To ensure the test stayed at room temperature, the IR sensor was fed into a control system which would stop the test should the specimen exceed 30 °C. The cooling pause would then be increased and the test started again. Photos of the test setup are shown in Figure 2 (a) and (b).

The low-frequency testing was carried out at 20 Hz using an Instron 8801 servohydraulic testing machine. The testing was carried out in environmental conditions and at room temperature, to keep all environmental influences consistent between the two tests. A photo of the test setup is shown in Figure 2 (c).

4. Results and discussion

4.1. Fatigue Results

The SN curves produced for Q355B at 20 Hz and 20 kHz are presented in Figure 3. The SN curves produced at low frequency show a good correlation with the traditional power law equation, however no clearly defined fatigue limit can be observed, as one specimen ran out at 300 MPa and another specimen failed at 270 MPa. The UFT curve exhibits a large amount of scatter in the data, with an R^2 value of 0.4264 when fitting to a power law curve. Additionally, all of the tested samples failed and so a fatigue limit value cannot be determined. This large amount of scatter in the fatigue results is to be expected based on the manufacturer's experience.

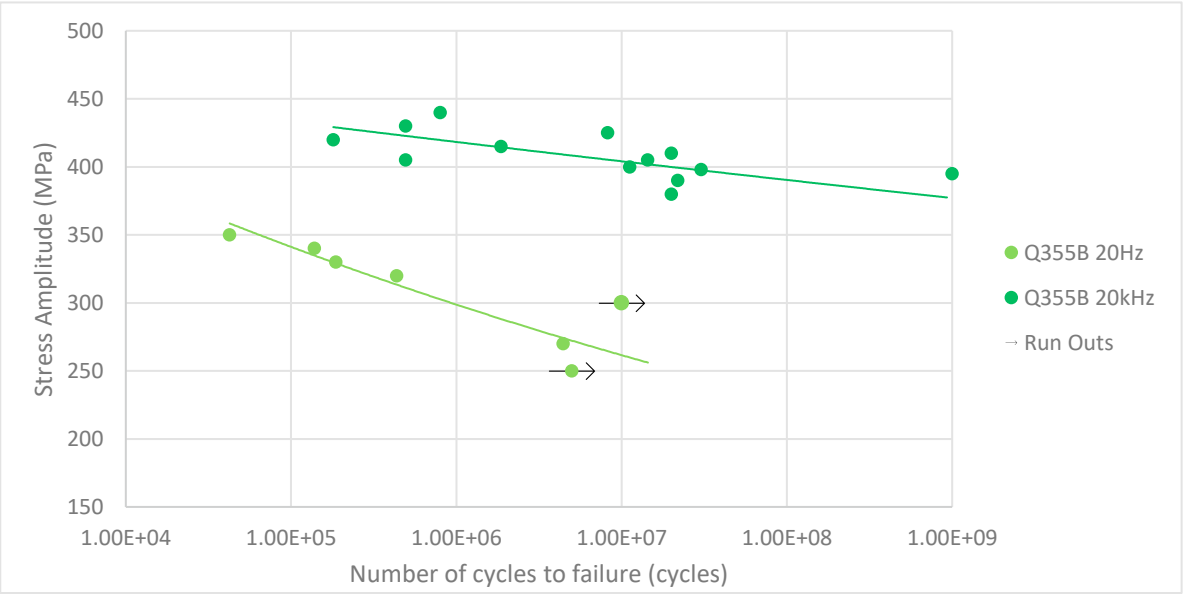

Figure 3: SN curves at 20 Hz and 20 kHz for Q355

As expected for a low-carbon steel, a significant discrepancy between the SN curves at the two frequencies can be observed. To quantify this discrepancy, the average difference in stress amplitude between the two SN curves was evaluated using the power law trendlines. The lower and upper bounds for this comparison were taken as the lowest value in the 20 kHz results and the highest value in the low-frequency results respectively. Using this method, the average discrepancy between the fatigue curves was determined to be 118.4 MPa, with the maximum difference being 136.2 MPa at $4.4x10^6$ cycles, and the minimum difference being 100.6 MPa at $1.8x10^5$ cycles.

For verification, the results were compared to similar materials tested in literature. Comparing to the steel grade Q345, as tested by Liu et al. (2016), a similar level of scatter is observed in the ultrasonic testing results. This confirms that this level of scatter is common among these grades. Additionally, a similar difference between the two SN curves can be extracted from their results, with an average difference of 112 MPa, and a difference range of 101 MPa – 123 MPa. This discrepancy closely matches the discrepancy observed for Q355B in this study.

The results were also compared to those produced by Klusák et al. (2021) for two different subgrades of an equivalent steel; S355J0 and J2. For this steel, there was significantly less scatter in the results, and a slightly higher strain rate sensitivity was observed, with an average discrepancy of 125 MPa and 128 MPa for the subgrades J0 and J2 respectively.

It can therefore be seen that the results match well when compared with those from literature, and the discrepancy between frequencies seems largely consistent across these similar grades of steel. The small differences in frequency sensitivity between the grades likely come from differences in test parameters, such as differences in the specimen geometries and test frequencies used for low-frequency testing.

4.2. Internal Heat Generation

For all of the tested samples, there was significant heat generation despite the attempts to overcome this. Although many of the samples started with a small temperature increase of 2-3 °C, the heat generation in each loading pulse would increase as the test progressed, to the point where it was exceeding the threshold of 30 °C with every loading pulse, even when using air cooling and applying the maximum cooling pause of 5 seconds. Beyond this point, it was no longer possible to keep the test below 30 °C. After this point, the test was continued with the specimen being allowed to heat up, and the peak temperature during each loading pulse was monitored. The temperature peaks with each loading pulse continued gradually increasing as the experiment continued, until just before failure when there was a large spike in temperature generation for all of the samples, due to the heat contribution from crack tip plasticity. This peak temperature spike ranged from 70 °C to 160 °C, and was generated from a single load pulse. The magnitude of the final peak temperature did not appear to correlate to the stress amplitude, although this could be due to the sampling rate of 20 ms being too low to capture the true peak temperatures during the 110 ms load pulses.

Discolourations were observed on the fracture surfaces of some of the samples tested at 395MPa and above, caused by intense localized heating at the crack tip. The size and severity of these discolourations did not appear to correlate with the stress amplitude or the fatigue life of the samples. Images of fracture surfaces showing these discolourations are presented in Figure 4.

This shows a limitation of ultrasonic fatigue testing of ferritic steels, as the magnitude of the heat generation at amplitudes around 400 MPa and above is so great that the specimen cannot be reasonably kept at room temperature. Additionally, intensive localized heating will occur once the fatigue crack starts propagating, which may influence the material's behaviour.

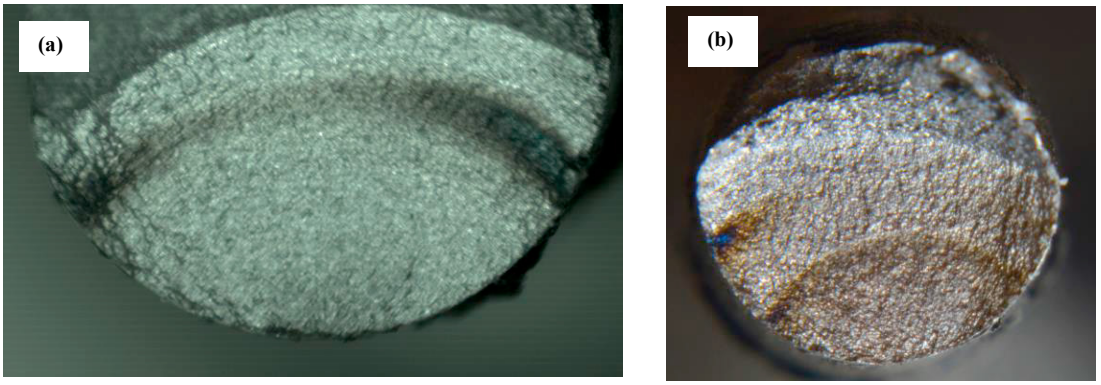

Figure 4: Images of the discolouration on the fracture surfaces of (a) 425 MPa sample, taken via optical microscopy and (b) 415 MPa sample, taken via macro photography

4.3. Fracture Origin

In all cases, the fracture originated from the surface of the specimens, even for specimens which failed in the VHCF regime. An example of the typical fracture surface is shown in Figure 5. No cracks originated from defects or inclusions within the bulk of the material, despite this commonly being considered to be a characteristic of VHCF failure. Comparing this observation to other low-carbon steels in literature, however, surface fracture origination remains a common source of failure even in the VHCF regime (Guennec et al. 2014; Nonaka et al. 2014). In the similar steel grades Q345 and S355 previously discussed, all fractures also originated from the surface (Klusák et al. 2021; Liu et al. 2016).

This observation was discussed by Torabian et al. (2017), who proposed that the transition to subsurface inclusion-induced crack initiation will only occur for ferritic materials which are loaded in the athermal deformation regime, whereas most of the ferritic steels tested at ultrasonic frequencies lie within the thermally activated glide regime. To illustrate this, a map of the deformation glide and fracture initiation mechanisms as a function of the strain rate and temperature was produced (Torabian et al. 2017). For the Q355 steel in this investigation, a nominal strain rate and temperature of $300s^{-1}$ and 300K can be assumed, which would put the initiation behaviour in the "surface failure from crack initiations at the grain boundaries" regime of the map, which agrees with the observed failure mode in the tested specimens.

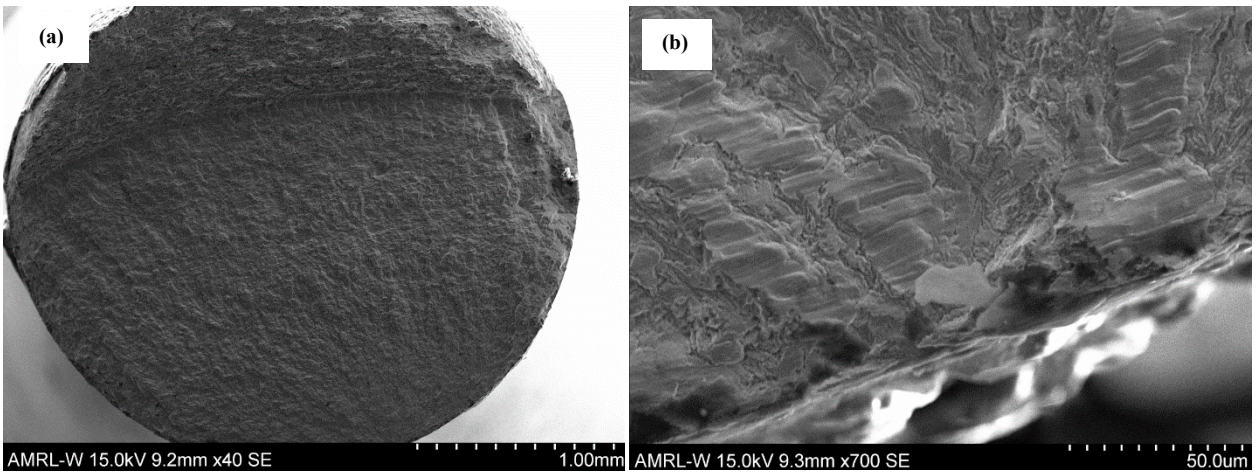

Figure 5: SEM images taken of (a) the fracture surface and (b) the fracture origin of a sample which failed at $2x10^7$ cycles

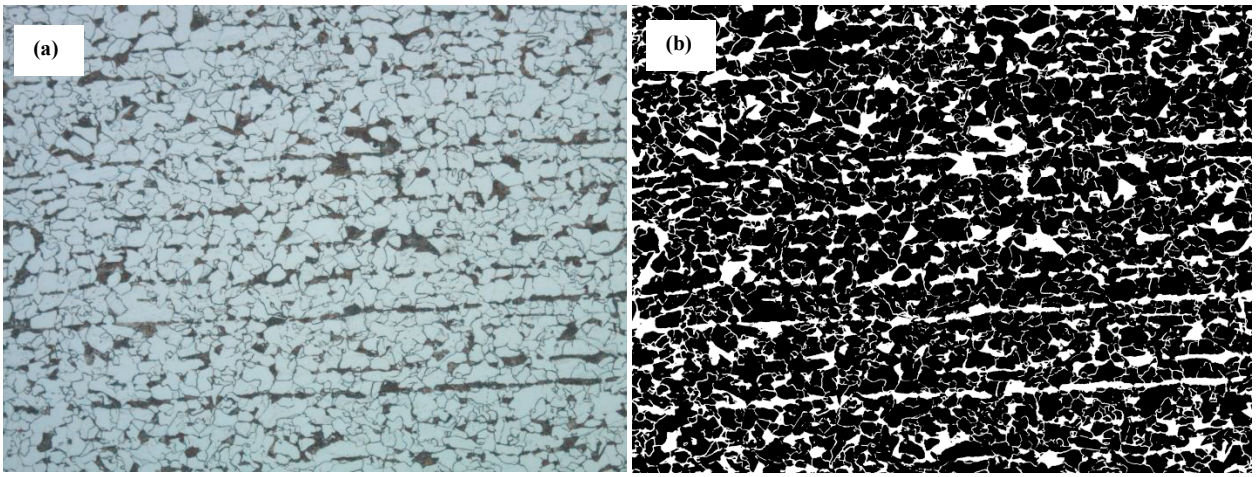

Figure 6: (a) Micrograph section of Q355B and (b) the same section with the ferrite regions highlighted in black

4.4. Effect of Ferrite Content on Frequency Sensitivity

It has been proposed that the ferrite volume content is one of the driving factors that significantly influence the strain rate sensitivity of carbon steels (Bach et al. 2018). As such, it is important to evaluate the ferrite content when investigating the strain rate sensitivity in steels. To evaluate the ferrite content of the Q355B steel, micrographs were taken from random points on the specimens at a magnitude of 200x, and image analysis was applied to determine the volume content of the ferrite and pearlite phases following the procedure given in ASTM E1245-03 (2016). An example of this procedure is given in Figure 6. This was carried out for eight sections and the results were averaged to mitigate any variability in the microstructure across the samples. Using this method, the ferrite volume content was evaluated to be approximately 75%. This is only an approximate value, however, as the exact threshold to use in the image analysis was difficult to determine precisely, and influenced the results by several %. In future, these results will be verified using other ferrite evaluation methods to ensure accurate measurements.

This analysis was also carried out for the steel S275JR, which was previously investigated under the same test conditions by the co-authors Gorash et al. (2022). The ferrite volume content in S275JR was evaluated as 81%, and the average discrepancy between the ultrasonic and standard frequency SN curves was evaluated as 170 MPa. As both the strain rate sensitivity and ferrite content were higher for S275JR, it would match the observations in literature that strain rate correlates with ferrite content.

5. Summary

The conclusions from this investigation are as follows:

- Test specimens were developed for Q355B which allowed fatigue testing at 20 Hz and 20 kHz frequencies with the same gauge section geometry. Specimens were successfully tested at both frequencies, although there was significant scatter in the ultrasonic data.
- The discrepancy observed between the fatigue data at the two frequencies matches well with similar steels tested in literature.
- The temperature of the UFT specimens could not be kept around room temperature, even with air cooling and the maximum cooling pause applied. Temperatures would increase up to 160 °C from a single cooling pulse just before failure and evidence of intense localized heating at the crack fronts could be observed on the fracture surfaces.
- All failures originated at the specimen surface and not from internal inclusions, which matches the expectations from literature for these loading conditions.

- Compared to steel S275JR as previously investigated, Q355B exhibits both a lower ferrite content and frequency sensitivity. This matches the proposal in literature that the increased ferrite content leads to greater frequency sensitivity.

Acknowledgements

The authors would like to acknowledge the support for this study, which was provided by the Weir Group PLC (WARC2011-SAA1, 2011) via its establishment of the Weir Advanced Research Centre (WARC) at the University of Strathclyde.

References

ASTM International, 2016. *ASTM E1245-03: Standard Practice for Determining the Inclusion or Second-Phase Constituent Content of Metals by Automatic Image Analysis*. West Conshohocken.

Bach, J., M. Göken, and Heinz-Werner Höppel, 2018. Fatigue of Low Alloyed Carbon Steels in the HCF/VHCF-Regimes, In "*Fatigue of Materials at Very High Numbers of Loading Cycles,*" H.-J. Christ (Ed.). Springer Fachmedien Wiesbaden, pp. 1–23.

Bathias, Claude, 2006. Piezoelectric Fatigue Testing Machines and Devices. Int. J. Fatigue 28 (11): 1438–45.

Fitzka, Michael, Bernd M. Schönbauer, Robert K. Rhein, Niloofar Sanaei, Shahab Zekriardehani, Srinivasan Arjun Tekalur, Jason W. Carroll, and Herwig Mayer, 2021. Usability of Ultrasonic Frequency Testing for Rapid Generation of High and Very High Cycle Fatigue Data. Materials (Basel). 14 (9).

Gorash, Yevgen, Tugrul Comlekci, Gary Styger, James Kelly, and Frazer Brownlie, 2022. Investigation of S275JR+AR Structural Steel Fatigue Performance in Very High Cycle Domain. Procedia Struct. Integr. 38 : 490–96.

Guennec, Benjamin, Akira Ueno, Tatsuo Sakai, Masahiro Takanashi, and Yu Itabashi, 2014. Effect of the Loading Frequency on Fatigue Properties of JIS S15C Low Carbon Steel and Some Discussions Based on Micro-Plasticity Behavior. Int. J. Fatigue 66 : 29–38.

Guennec, Benjamin, Akira Ueno, Tatsuo Sakai, Masahiro Takanashi, Yu Itabashi, and Mie Ota, 2015. Dislocation-Based Interpretation on the Effect of the Loading Frequency on the Fatigue Properties of JIS S15C Low Carbon Steel. Int. J. Fatigue 70 : 328–41.

Hu, Yuanpei, Chengqi Sun, Jijia Xie, and Youshi Hong, 2018. Effects of Loading Frequency and Loading Type on High-Cycle and Very-High-Cycle Fatigue of a High-Strength Steel. Materials (Basel). 11 (8).

Klusák, Jan, Vít Horník, Grzegorz Lesiuk, and Stanislav Seitl, 2021. Comparison of High- and Low-Frequency Fatigue Properties of Structural Steels S355J0 and S355J2. Fatigue Fract. Eng. Mater. Struct. 44 (11): 3202–13.

Liu, Hanqing, Qingyuan Wang, Zhiyong Huang, and Zhenjie Teng, 2016. High-Cycle Fatigue and Thermal Dissipation Investigations for Low Carbon Steel Q345. Key Eng. Mater. 664 : 305–13.

Mughrabi, H., K. Herz, and X. Stark, 1981. Cyclic Deformation and Fatigue Behaviour of α-Iron Mono-and Polycrystals. Int. J. Fract. 17 (2): 193–220.

Nonaka, Isamu, Sota Setowaki, and Yuji Ichikawa, 2014. Effect of Load Frequency on High Cycle Fatigue Strength of Bullet Train Axle Steel. Int. J. Fatigue 60 : 43–47.

The Japan Welding Engineering Society, 2017. *WES 1112:2017 Standard Test Method for Ultrasonic Fatigue Testing of Metallic Materials*. Tokyo, Japan.

Torabian, Noushin, Véronique Favier, Justin Dirrenberger, Frédéric Adamski, Saeed Ziaei-Rad, and Nicolas Ranc, 2017. Correlation of the High and Very High Cycle Fatigue Response of Ferrite Based Steels with Strain Rate-Temperature Conditions. Acta Mater. 134 : 40–52.

Tsutsumi, Noriko, Y. Murakami, and V. Doquet, 2009. Effect of Test Frequency on Fatigue Strength of Low Carbon Steel. Fatigue Fract. Eng. Mater. Struct. 32 (6): 473–83.